

19. W. J. Welch and J. R. Feramisco, unpublished data.
20. Y. Kozutsumi, M. Segal, K. Normington, M. J. Gething, J. Sambrook, *Nature* **332**, 462 (1988); T. Nakaki, R. J. Deans, A. S. Lee, *Mol. Cell Biol.* **9**, 2233 (1989).
21. K. Riabowol, L. A. Mizzen, W. J. Welch, *Science* **242**, 433 (1988).
22. For preparation of polysomes, each 10-cm dish of [<sup>35</sup>S]Met-labeled HeLa cells was harvested as in Fig. 3 in a total volume of 1 ml. The 20,000g supernatant was layered onto an 11.5-ml continuous gradient of 0.5M to 1.5M sucrose in 10 mM Hepes-KOH pH 7.4, 5 mM MgCl<sub>2</sub> and 100 mM KCl. Gradients were centrifuged in an SW41 rotor (Beckman) at 100,000g for 2 hours at 8°C, and fractionated into 24 samples (0.5 ml). Absorbance at 254 nm was determined for each fraction in a model DU-65 spectrophotometer (Beckman).
23. M. M. Bradford, *Anal. Biochem.* **72**, 248 (1976).
24. E. Harlow and D. Lane, *Antibodies: A Laboratory Manual* (Cold Spring Harbor Laboratory, Cold Spring Harbor, NY, 1988).
25. R. J. Ellis, *Nature* **328**, 378 (1987).
26. We thank many colleagues for discussion and encouragement: R. Voellmy, J. Feramisco, V. Lingappa and his colleagues; T. Fink, C. Georgopoulos, and members of the Lung Biology Center; T. Kleven for preparation of the manuscript; and M. Lovett for technical assistance. Supported by NIH grant GM 33551 (to W.J.W.), MRC fellowship (Canada) (to L.A.M.), and the Department of Medicine, UCSF (R.P.B.).

16 January 1990; accepted 11 April 1990

**Table 1.** Patient information. Abbreviations: AD, Alzheimer's disease; PD, idiopathic Parkinson's disease; and MID, multi-infarct dementia.

Case number	Age	Sex	Diagnosis
1	90	F	AD
2	85	F	AD
3	87	M	AD
4	82	M	AD
5	81	F	AD
6	70	F	AD
7	78	M	AD/PD
8	88	M	PD
9	69	M	PD
10	78	M	PD/MID
11	66	M	Normal

## Relation of Neuronal APP-751/APP-695 mRNA Ratio and Neuritic Plaque Density in Alzheimer's Disease

STEVEN A. JOHNSON, THOMAS MCNEILL, BARBARA CORDELL, CALEB E. FINCH

An ongoing controversy concerns the cellular distribution of the differentially spliced forms of the amyloid protein precursor (APP) mRNAs and changes in prevalence of these transcripts during Alzheimer's disease. In situ hybridization on serial sections was used to prove that most hippocampal pyramidal neurons contain both APP-751 and APP-695 mRNA species. The APP-751/APP-695 mRNA ratio is generally increased during Alzheimer's disease, as shown by RNA gel blot analysis. Moreover, there was a strong linear relation between the increase in APP-751/APP-695 mRNA ratio in pyramidal neurons and the density of senile plaques within the hippocampus and entorhinal cortex. Thus, the increase in APP-751/APP-695 mRNA provides a molecular marker for regional variations in plaque density between individuals diagnosed with Alzheimer's disease by the commonly used composite criteria.

ACCUMULATIONS OF  $\beta$  amyloid in neuritic plaques and cerebral blood vessels are characteristic of Alzheimer's disease (AD). One hypothesis concerns the relation between altered proteolytic activity and  $\beta$ -amyloid deposition in plaques. The mRNA for amyloid protein precursor (APP) in aged human brain consists of two major alternatively spliced forms, APP-695 and APP-751; the latter has an exon encoding a Kunitz-type serine protease inhibitor (KPI) (1-3). Several other alternatively spliced or truncated KPI-containing APP mRNA forms (APP-770 and APP-543) are known (3), but are rare in aged human brain. APP-751 may be identical to the serine protease inhibitor protease nexin-II, on the basis of the available NH<sub>2</sub>-terminal sequence (4, 5). Extracts of cells transfected with APP-770 have trypsin inhibitory activity (6). The APP is axonally transported and localized to synaptic mem-

branes (7-10). An increase in the ratio of KPI-APP mRNA/APP-695 mRNA during AD could alter local membrane proteolytic activity and play a role in  $\beta$ -amyloid deposition and plaque formation. A major question is the distribution of each APP mRNA form with respect to local accumulations of amyloid.

Using probes specific for each APP RNA, we (11, 12) and others (2, 13) showed that the APP-751/APP-695 mRNA ratio increased in hippocampal and neocortical tissues during AD. In contrast, an indirect assay by in situ hybridization (14) indicated that APP-695 mRNA was increased in the nucleus basalis and locus ceruleus of individuals with AD. However, present data do not indicate whether there is a selective loss of neurons with high prevalence of a particular APP mRNA. It is therefore crucial to measure the neuronal prevalence of each APP transcript and to establish if both APP mRNA forms are present in the same neurons to understand the possible relation between changes in APP mRNAs and AD.

In situ hybridization with APP-751- and APP-695-specific probes (15) was performed on adjacent serial hippocampal sec-

tions from seven clinically and pathological confirmed AD and four non-AD individuals. Neuronal grain density was determined by computer-assisted image analysis, and a comparative bridge microscope was used to colocalize the presence of each APP transcript in the same neuron from adjacent tissue sections (16, 17).

The APP-751/APP-695 grain density ratio was twofold higher in each subfield of AD hippocampus compared to non-AD hippocampus (Fig. 1 and Tables 1 and 2). The majority (five out of seven) of AD individuals had APP-751/APP-695 ratios that were higher than the four controls. Data presented show that specific regions of an AD brain may not show increased APP-751/APP-695 mRNA ratios if that region has low plaque density. We also found that individual pyramidal neurons contain both APP-695 and APP-751 mRNAs, by comparing identical cellular fields from adjacent sections (Fig. 2). Most (97%;  $n = 104$ ) neurons common to both adjacent sections show cytoplasmic hybridization in the AD and non-AD specimens examined.

Neuronal loss and atrophy is common in AD, especially in hippocampal pyramidal fields (18). Because Northern (RNA) blot data have shown an increased APP-751/APP-695 mRNA ratio in hippocampus (12), it was important to determine whether this resulted from a loss of neurons that selectively contain APP-695 mRNA. Thus, we counted all neurons that hybridized to either APP-751- or APP-695-specific probes in adjacent tissue sections. The data are expressed as a ratio of neurons that contain 751 mRNA or 695 mRNA and show that the ratio of hippocampal pyramidal neurons containing each APP mRNA did not differ significantly between AD or non-AD individuals (Fig. 3).

Analysis across individuals showed a strong relation between the APP-751/APP-695 mRNA ratio and plaque density by Bielschowsky staining in the hippocampus

S. A. Johnson, T. McNeill, C. E. Finch, Andrus Gerontology Center, University of Southern California, Los Angeles, CA 90089.

B. Cordell, California Biotechnology, 2450 Bayshore Parkway, Mountain View, CA 94043.

**Table 2.** Regional grain density measurements for each individual. Density was defined and determined as in Fig. 1. Significance levels for *t* test of difference between AD and CTL were as follows. For APP-751-specific probe: CA3, *P* = 0.10; CA1, *P* = 0.06; and subiculum, *P* = 0.06. For APP-695-specific probe: CA3, *P* = 0.98; CA1, *P* = 0.81; and subiculum, *P* = 0.90. Abbreviations: CTL, control; ND, not determined.

CA3		CA1		Subiculum	
AD	CTL	AD	CTL	AD	CTL
<i>APP-751-specific probe</i>					
9.51	9.04	9.73	9.70	10.90	9.55
7.90	5.48	6.77	3.38	5.32	2.69
10.08	3.77	9.40	3.02	12.07	2.03
ND	2.56	9.42	2.89	8.73	2.78
6.82		6.94		7.62	
4.53		5.20		4.32	
12.57		13.00		10.67	
Average ± SEM					
8.57 ± 1.15	5.23 ± 1.20	8.63 ± 0.97	4.75 ± 1.65	8.51 ± 1.12	4.27 ± 1.78
<i>APP-695-specific probe</i>					
5.59	9.11	4.30	9.82	5.21	10.79
4.00	6.72	3.25	4.30	3.46	4.67
7.70	4.98	6.75	4.39	6.19	3.76
ND	3.01	4.05	3.64	4.00	2.78
1.97		2.83		3.24	
5.93		5.54		7.37	
13.42		16.32		10.94	
Average ± SEM					
6.43 ± 1.60	6.38 ± 1.66	6.16 ± 1.76	5.52 ± 1.44	5.77 ± 1.03	5.53 ± 1.80

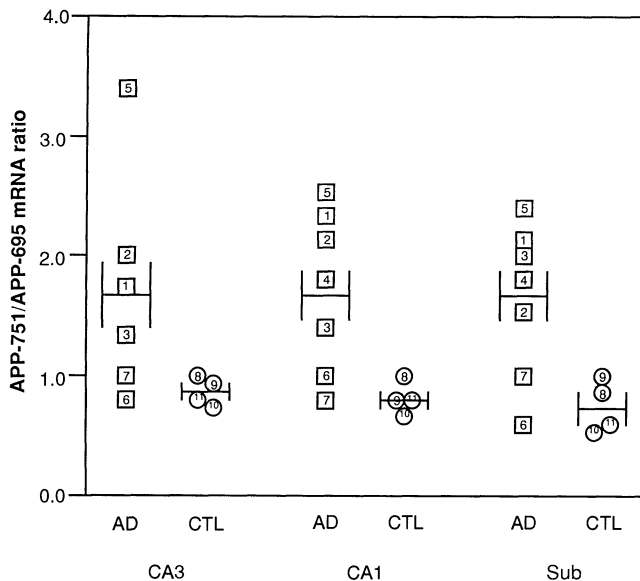


**Fig. 1.** APP-751/APP-695 grain density ratio is increased in hippocampal pyramidal neurons from CA3, CA1, and subicular (Sub) subfields during AD. The APP-695- or APP-751-specific grain densities were determined after high criterion, serial section in situ hybridization (27) on hippocampal sections of seven AD and four non-AD individuals. The 30-nt cRNA APP-695- or APP-751-specific antisense and sense strand cRNA probes (15) were synthesized concomitantly and were of equal specific radioactivity ( $6 \times 10^9$  dpm/ $\mu$ g). Sections were processed, hybridized, washed, and exposed together (28). The silver grain density (area covered by

grains divided by total cellular area) over labeled neurons was determined by computer with a grain counting software package (Southern Micro, Atlanta, Georgia). Background was monitored for each specimen by hybridization of an adjacent section to a 30-nt J-24 cRNA sense strand probe synthesized identically to the antisense probes. The stringent wash criterion ( $T_m - 10^\circ\text{C}$ ) resulted in low background with no specific perikaryal signal above minimal acellular background with this sense strand control. Thus, background was measured in acellular areas within the pyramidal cell field of slides hybridized to antisense probes. Squares represent AD individuals and circles represent control (CTL) individuals. To determine the minimal number of neurons that would yield statistically accurate data, we measured the grain density of every labeled pyramidal neuron in CA3, CA1, and subiculum of one APP-751 and one APP-695 hybridized section each from one AD and one non-AD individual (four sections). Then different-sized subsets of 30, 50, and 100 neurons were randomly selected, and the means of these random data sets were compared to the mean of the entire data set for each region in each section. Thirty neurons yielded a mean that was statistically equivalent to the overall mean (*t* test, *P* = 0.05). Thus, we generally counted 50 or more neurons per field in CA3, CA1, and subiculum of the remaining slides. All slides were randomly coded before cell count and grain density analyses so the observer did not know the probe used or the disease status. The number inside each symbol refers to the individual case number, as shown in Table 1. The mean ± SEM is shown for each data set. CA3 from individual number 4 was not available for analysis. Statistical analysis showed the mean APP-751/APP-695 ratios were significantly different between AD and control for CA1 and subiculum, but not for CA3 (unpaired *t* test; CA1, *t* = 2.55, *P* < 0.05; Sub, *t* = 2.60, *P* < 0.05; CA3, *t* = 1.69, *P* = 0.13).

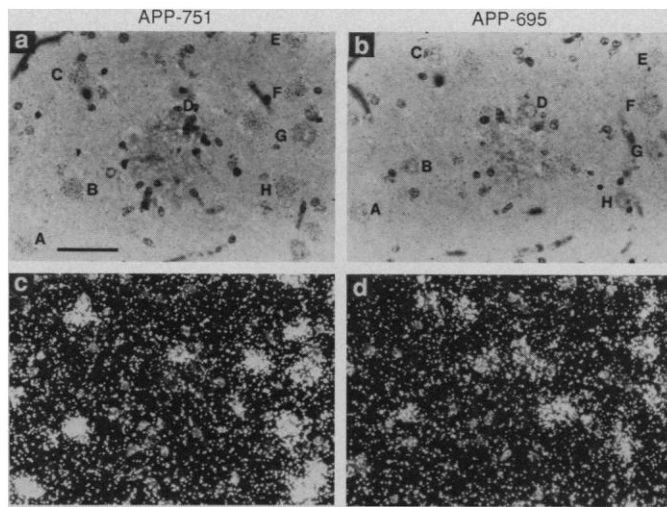
and entorhinal cortex (Fig. 4). There are several instructive individual variations in the AD brains. Case number 4 had few plaques in the entorhinal cortex, yet abundant plaques in the hippocampus; case 6 was the converse. Case 7 had a few plaques in hippocampus, several in entorhinal cortex, and low APP-751/APP-695 mRNA ratios in these regions. The diagnosis of AD for case 7 was based on clinical history and the presence of plaques in frontal and temporal cortex. Thus, an mRNA change in a brain region during AD was linearly related with neuritic plaque density.

The AD-specific increase in the hippocampal pyramidal neuron APP-751/APP-695 ratio is primarily due to an increase in APP-751 transcript, with no change (unpaired *t* test, *t* = 0.36, *P* = 0.72, not significant) in neuronal APP-695 mRNA prevalence (3). This differs from previous results obtained by RNA gel blot analyses, which showed a small increase in APP-751 mRNA together with a large decrease in APP-695 mRNA in AD neocortex and hippocampus. It is difficult to compare these two methods of RNA prevalence analysis because our study measured neuronal RNA specifically by in situ hybridization, whereas RNA gel blot analysis measures bulk RNA from all cells. Although the cause of the difference between studies is unclear, our Northern blot data (11, 12) are consistent with other reports (2, 13).

Furthermore, a recent abstract (19) corroborated the increase of APP-751 mRNA by in situ hybridization in AD hippocampus reported here and further documented an increased APP-751/APP-695 mRNA ratio in AD nucleus basalis. Thus, although these recent data [from our study and (19)] are in agreement, they conflict with a previous report (14), which showed a decreased APP-751/APP-695 mRNA ratio in AD nucleus basalis and little change in AD subiculum. In (14), APP-695 mRNA prevalence was only measured indirectly by subtracting KPI-specific probe signal from total APP mRNA signal obtained with a 3' APP probe common to all APP mRNAs. Moreover, unlike the present study, in (14) the KPI-specific and total APP probes had different lengths and specific radioactivity, and tissue sections hybridized with each probe were exposed for different times. These procedural differences further complicate the estimation of APP-695 and APP-751 mRNA prevalence by this indirect method.

Two mechanisms might alter the steady-state ratio of alternatively spliced APP transcripts—regulation of differential splicing or of differential mRNA stability. In regulation of mRNA stability, two factors are known. First, the removal or replacement of a 63-

**Fig. 2.** Both APP-751 and APP-695 mRNAs coexist in the same AD hippocampal pyramidal neurons. (a and b) Bright-field photomicrographs of the identical location (pyramidal layer, CA3/CA4 boundary) from adjacent serial sections of AD individual 5, which were hybridized to I-22 (APP-751) and J-24 (APP-695) probes (15), respectively. (c and d) Dark-field photomicrographs of the same fields in (a) and (b), respectively. Neurons labeled A to H in (a) and (b) represent the same neurons in the alternate serial sections that show hybridization to both APP probes. The image in (b) is rotated approximately 15° clockwise in relation to (a). There is greater grain density over neurons hybridized to I-22 (APP-751-specific), compared to the same neurons after hybridization to J-24 (APP-695-specific). We used two Leitz microscopes connected with a comparative bridge to locate a number of different areas in the hippocampal pyramidal layer that had numerous neurons common to both adjacent sections, as judged by the ability of the observer to overlay many neurons from each section by eye in the comparative bridge microscope. A number of different areas in different hippocampal subfields of various individuals were photographed. Photocopied transparencies of enlargements were overlaid on the enlargement of the same area in the adjacent section, and common neurons with grain density above background were counted. Scale bar, 10  $\mu$ m.



nucleotide (nt) 3' untranslated AU-rich sequence increased the stability of *c-fos* mRNA in transfected NIH 3T3 cells (20). Second, Yen *et al.* (21) showed that the NH<sub>2</sub>-terminal amino acid sequence controls the auto-regulated instability of  $\beta$  tubulin. However, neither of these factors applies to the APP mRNA family, since there are no known differences in the 3' untranslated or 5' coding sequences between the various alterna-

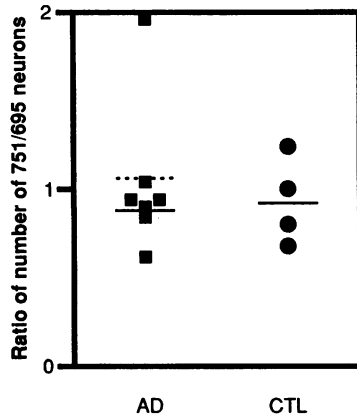


**Fig. 3.** Ratio of the number of hippocampal pyramidal neurons detected by APP-695- or APP-751-specific probes. Adjacent serial sections were hybridized to either APP-751- or APP-695-specific probes. Nucleolated pyramidal neurons (>700 neurons per section per individual) were counted with the aid of an ocular grid, by using obvious landmarks to ensure the same cellular field was counted in each adjacent section. Means are not significantly different by paired *t* test. AD: APP-751 versus APP-695,  $P > 0.68$ ; CTL: APP-751 versus APP-695,  $P > 0.67$ .

tively spliced APP mRNAs in AD versus non-AD (1, 22-24). Thus, it seems unlikely that differential APP mRNA stability is responsible for the increased APP-751/APP-695 mRNA ratio in AD hippocampus. On

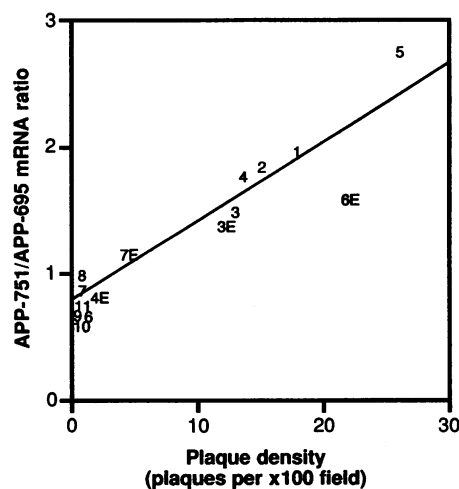


**Fig. 4.** Relation of the APP-751/APP-695 mRNA ratio in neurons from individual hippocampal and entorhinal cortex specimens with amyloid plaque density in that region (slope  $\pm$  SE =  $0.06 \pm 0.01$ ,  $t = 9.18$ ,  $P < 0.001$ ). The specimen numbers refer to Table 1; the entorhinal cortex (E) from various individuals are included in the analysis because some of these individuals had low APP-751/APP-695 mRNA ratios and low plaque density in the hippocampus, whereas others had low APP mRNA ratio and plaque density in the entorhinal cortex and higher ratios and plaque density in the underlying hippocampus.

the other hand, sexual differentiation in *Drosophila* is controlled by differential splicing of the *Drosophila* "sex-lethal" gene product (25), possibly through an RNA binding protein that regulates the alternative splicing event (26). Changes in such an RNA binding protein could regulate alternative splicing of the APP nuclear RNA and alter the APP-751/APP-695 mRNA ratio in AD neurons.

In conclusion, we showed a twofold increase in the neuronal APP-751/APP-695 mRNA ratio in AD versus non-AD hippocampus by *in situ* hybridization. This increase is not due to decreased numbers of neurons that only contain APP-695 mRNA because equivalent numbers of hippocampal pyramidal neurons hybridized independently to APP-695- and APP-751-specific probes. Furthermore, we provide evidence that each pyramidal neuron contains both APP-695 and APP-751 mRNAs.

Together, these data suggest that changes in APP mRNA abundance arise posttranscriptionally and may be due to altered APP nuclear RNA splicing in neurons of affected regions of the AD brain. These findings (11-13) show changes in prevalence of alternatively spliced mRNAs during an adult neurodegenerative disease. In addition, the strong relation between plaque density and pyramidal APP mRNA ratio indicates that the increased APP-751/APP-695 mRNA ratio relates better with neuritic plaque density in that brain region than with the global diagnosis of AD. The question is open about how the APP mRNA ratio relates to the functional expression of each encoded protein and the mechanism of amyloid deposition in AD. In view of the axonal transport of APP peptides (7), the relative increase of APP mRNA that encodes the serine protease inhibitor could be a factor in the abnormal accumulation of  $\beta$  amyloid in that region. The present data thus support and further specify the original proposals that the KPI domain was important in amyloid accumulation during AD (2, 6).

#### REFERENCES AND NOTES

1. P. Ponte *et al.*, *Nature* 331, 525 (1988).
2. R. E. Tanzi *et al.*, *ibid.*, p. 528.
3. We (12) found, in agreement with others [G. Konig, J. M. Salbaum, C. L. Masters, K. Beyreuther, *Alzheimer Dis. Assoc. Disord.* 2, 347 (1988)], that the cortical APP-770 (6) transcript prevalence represents <5% of total APP mRNA in AD, after a twofold increase over the control level of 2 to 3% of total APP transcript; thus the KPI-specific signal in this study is predominantly APP-751 mRNA. F. de Sauvage and J. N. Octave [*Science* 245, 651 (1989)] cloned from AD cortex a truncated KPI-containing APP mRNA, APP-543, which lacks sequence information for the COOH-terminal 208 amino acids of APP-751. This novel form is present in trace amounts, which we did not detect during previous Northern blot analyses of AD or control polyade-

- nylated RNA (11, 12).
4. W. E. Van Nostrand *et al.*, *Nature* **341**, 546 (1989).
  5. T. Oltersdorf *et al.*, *ibid.*, p. 144.
  6. N. Kitaguchi *et al.*, *ibid.* **331**, 530 (1988).
  7. E. H. Koo *et al.*, *Soc. Neurosci. Abstr.* **14**, 23 (1989).
  8. B. D. Shivers *et al.*, *EMBO J.* **7**, 1365 (1988).
  9. T. Dyrks *et al.*, *ibid.*, p. 949.
  10. A. Weidemann *et al.*, *Cell* **57**, 115 (1989).
  11. S. A. Johnson *et al.*, *Exp. Neurol.* **102**, 264 (1988).
  12. S. A. Johnson, J. Rogers, C. E. Finch, *Neurobiol. Aging* **10**, 267 (1989).
  13. R. L. Neve, E. A. Finch, L. R. Dawes, *Neuron* **1**, 669 (1988).
  14. M. R. Palmert *et al.*, *Science* **241**, 1080 (1988).
  15. J-24 is a recombinant pGEM 1 vector containing the sequence AAGAG GTGGT TCGAG TTCCT ACAAC AGCAG [APP nt 975–989 + nt 1158–1172 (1)] that was used to synthesize a 30-nt antisense junctional probe which only hybridizes to APP-695, since the 168-nt KPI exon in APP-751/APP-770 splits the J-24 complement in half and prevents J-24 hybridization at stringent criterion (11, 28). Similarly, I-22 is a recombinant pGEM 1 vector containing AAGGG AAGTG TGCCC CATTCTTTTA CGGCG [APP nt 1062–1091 (1)] that was used to synthesize a KPI insert-specific probe which hybridizes only to APP-751/APP-770. The synthesis and characterization of sense and antisense 30-nt RNA probes specific for APP-751 and APP-695 mRNAs were described (11).
  16. T. H. McNeill and J. R. Sladek, *Brain Res. Bull.* **5**, 599 (1980).
  17. J. R. Sladek, C. D. Sladek, T. H. McNeill, J. G. Wood, in *Brain-Endocrine Interaction III: Neural Hormones and Reproduction*, Proceedings of the 3rd International Symposium, Wurzburg, July 1977, D. E. Scott, A. Weindl, G. P. Kozlowski, Eds. (Karger, Basel, 1978), pp. 154–171.
  18. P. D. Coleman and D. G. Flood, *Neurobiol. Aging* **8**, 929 (1987).
  19. R. L. Neve and G. A. Higgins, *Soc. Neurosci. Abstr.* **14**, 1378 (1989).
  20. T. Wilson and R. Treisman, *Nature* **336**, 396 (1988).
  21. T. J. Yen, P. S. Machlin, D. W. Cleveland, *ibid.* **334**, 580 (1988).
  22. J. Kang *et al.*, *ibid.* **325**, 733 (1987).
  23. S. B. Zain *et al.*, *Proc. Natl. Acad. Sci. U.S.A.* **85**, 929 (1988).
  24. M. P. Vitek *et al.*, *Mol. Brain Res.* **4**, 121 (1988).
  25. B. S. Baker, *Nature* **340**, 521 (1989).
  26. L. R. Bell, E. M. Maine, P. Schedl, T. W. Cline, *Cell* **55**, 1037 (1988).
  27. G. A. Higgins *et al.*, *Proc. Natl. Acad. Sci. U.S.A.* **85**, 1297 (1988).
  28. Paraffin sections (10  $\mu$ m) were deparaffinized in HistoClear, hydrated in descending graded ethanol solutions, fixed in fresh, buffered 4% paraformaldehyde (3 min, 25°C), treated with proteinase K (25  $\mu$ g/ml) in 50 mM Tris, 5 mM EDTA, pH 8.0, for 7 min at 25°C and in 0.05M HCl for 10 min at 25°C, and finally post-fixed in 4% paraformaldehyde (5 min, 25°C) before drying in ascending graded ethanols. Sections were rinsed twice in phosphate-buffered saline (0.1M sodium phosphate buffer (NaPB), pH 6.8, 0.9% NaCl) after each step of the treatment. Prehybridization was for 2 hours at 53°C in 50% redistilled formamide, 0.75M NaCl, 0.025M NaPB, pH 6.8, 10 mM EDTA, 1.0% SDS, 250 mM dithiothreitol (DTT), heparin (10  $\mu$ g/ml) [M. Goedert, *EMBO J.* **6**, 3627 (1987)], 5 $\times$  Denhardt's solution [0.1% each of bovine serum albumin, polyvinylpyrrolidone (PVP), and Ficoll], and purified transfer RNA (500  $\mu$ g/ml). Hybridization was for 3 to 4 hours at 53°C in prehybridization buffer plus 10% dextran sulfate and [<sup>35</sup>S]RNA probe (2  $\times$  10<sup>8</sup> cpm/ml). Slides were held on a warming plate at 53°C during addition of hybridization solution to rapidly initiate hybridization during probe addition and as cover slips were added to other slides. Cover slips were removed by soaking slides in 50% formamide, 0.75M NaCl, 0.025M NaPB, and 250 mM DTT. Washing involved a single, very stringent incubation in 200 ml of the above 50% formamide high-salt solution at 63°C [which is 10°C below the melting temperature ( $T_m$ )], for 30 to 60 min, followed by extensive washing overnight in a 2-liter solution of 0.5 $\times$  saline sodium citrate, and 20

mM 2-mercaptoethanol at 25°C. Slides were dried by passage through ascending ethanol solutions containing 0.3M ammonium acetate and coated with NTB-2 emulsion (Kodak). After a 4-month exposure at 4°C, the emulsion was developed according to manufacturer's directions and slides were counterstained lightly with cresyl violet.

29. We thank P. Ponte for I-22 and J-24 RNA probe construction; D. Morgan, P. Ponte, and J. Day for manuscript critique; and C. Zarow for helpful discussions. Tissue for this study was obtained from J.

Rogers, Institute for Biogerontology Research, Sun City, AZ, and from the Alzheimer's Disease Research Center of Southern California Autopsy Core. Supported by grants from the National Institute on Aging to C.E.F. (AG05142 and AG07909), and by California Biotechnology. S.A.J. was supported by a grant from the Alzheimer's Disease and Related Disorders Association.

20 November 1989; accepted 26 February 1990

## Genetic Suppression of Mutations in the *Drosophila* *abl* Proto-Oncogene Homolog

FRANK B. GERTLER, JOHN S. DOCTOR, F. MICHAEL HOFFMANN

The *Drosophila abelson (abl)* gene encodes the homolog of the mammalian *c-abl* cytoplasmic tyrosine kinase and is an essential gene for the development of viable adult flies. Three second-site mutations that suppress the lethality caused by the absence of *abl* function have been isolated, and all three map to the gene *enabled (ena)*. The mutations are recessive embryonic lethal mutations but act as dominant mutations to compensate for the neural defects of *abl* mutants. Thus, mutations in a specific gene can compensate for the absence of a tyrosine kinase.

THE CYTOPLASMIC TYROSINE KINASES were originally discovered as the products of oncogenes encoded by transforming retroviruses (1). The proto-oncogenic forms of cytoplasmic tyrosine kinases are expressed in normal cells and have been implicated in essential cellular processes, including cell proliferation and differentiation (2). To further understand the roles of cytoplasmic tyrosine kinases in cellular functions, we have isolated mutations in the *abelson (abl)* cytoplasmic tyrosine kinase of *Drosophila* (3) and examined the consequences to cell growth and development. Mutations in *abl* result in death of the animal during metamorphosis or in appearance of adults exhibiting a variety of mutant phenotypes, including roughened eyes, reduced longevity, and reduced fecundity. The *abl* protein can be detected by immunohistochemical methods in differentiating neural cells of the embryonic central nervous system (CNS) and the retinal cells of the eye.

We have isolated mutations that act as genetic enhancers and suppressors of the mutant phenotypes of *abl*. These mutations can be used to identify genes whose products act in the same biological processes as the *abl* cytoplasmic tyrosine kinase, and in some cases might identify genes whose products directly interact with the tyrosine kinase either as regulators of *abl* activity or as substrates for *abl*. One of the genetic enhancers is the *disabled (dab)* gene (4). Heterozygous mutations in *dab* act as dominant

genetic enhancers of the mutant phenotypes caused by homozygous *abl* mutations: a *dab* mutation shifts the mutant phenotype from pupal lethality to embryonic and early larval lethality. In animals homozygous mutant for both *abl* and *dab*, severe disruptions are observed in the axonal connections of the developing CNS (4).

We used a screening procedure to recover second-site mutations that would shift the lethal phase of animals homozygous mutant for *abl* and heterozygous mutant for *dab* from embryonic or larval stages back to the pupal stage. The strategy would detect dominant mutations on the second or third chromosomes, which account for 80% of the *Drosophila* genome (5). From 4000 mutagenized chromosomes, three independent mutations were recovered; each of the mutations not only compensated for the embryonic or larval lethality of the mutant animals, but also allowed recovery of fertile adult flies. All three mutations segregate with the second chromosome and map to chromosome arm 2R between the dominant visible mutations *Black cell (Bc)* and *Punch (Pu)* (6). Genetic analysis indicates that all three mutations are allelic (see below); we have named this complementation group *enabled (ena)*.

The characteristics of the *ena* mutations were tested in a number of different genetic backgrounds (Table 1). In animals mutant for *abl*, which would otherwise die as pupae, each of the three *ena* mutations acts in a dominant fashion to compensate for the absence of *abl* and allow recovery of fertile adults. Even the defective pattern of retinal

McArdle Laboratory for Cancer Research, University of Wisconsin, Madison, WI 53706.